

Orientation dependence of the anomalous Hall resistivity in single crystals of $\text{Yb}_{14}\text{MnSb}_{11}$

Brian C. Sales, Rongying Jin, and David Mandrus

Materials Science and Technology Division, Oak Ridge National Laboratory, Oak Ridge, Tennessee 37831, USA

(Received 18 July 2007; revised manuscript received 14 September 2007; published 10 January 2008)

The Hall resistivity, electrical resistivity, and magnetization of single crystals of the tetragonal ferromagnet $\text{Yb}_{14}\text{MnSb}_{11}$ are reported as a function of the direction of the current \mathbf{I} and magnetic field \mathbf{H} with respect to the principal crystallographic axes. With \mathbf{I} along the unique c direction and \mathbf{H} in the a - b plane, the anomalous Hall resistivity in the limit of zero applied field is negative for all temperatures $T < T_C = 53$ K. In this direction, the anomalous Hall effect behaves in a manner similar to that observed in other ferromagnets such as Fe, Co, Mn_5Ge_3 , and $\text{EuFe}_4\text{Sb}_{12}$. However, with \mathbf{I} in the a - b plane and \mathbf{H} along the c direction, the anomalous Hall behavior is completely different. The anomalous Hall resistivity data are positive for all $T < T_C$ and a similar analysis of these data fails. In this direction, the anomalous response is not a simple linear function of the magnetization order parameter, and for a fixed temperature, ($T < T_C$) does not depend on the magnitude of the magnetization perpendicular to the current in the a - b plane. That is, when the magnetization and applied field are rotated away from the c direction, the *anomalous Hall resistivity does not change*. In all other soft ferromagnets that we have examined (including La doped crystals of $\text{Yb}_{14}\text{MnSb}_{11}$, i.e., $\text{Yb}_{13.3}\text{La}_{0.7}\text{MnSb}_{11}$), rotation of the magnetization and magnetic field by an angle θ away from a direction perpendicular to \mathbf{I} results in a decrease in both the anomalous and normal portions of the Hall resistivity that approximately scales as $\cos(\theta)$. We suggest that the unique response exhibited by $\text{Yb}_{14}\text{MnSb}_{11}$ is a direct reflection of the delicate balance between ferromagnetism and Kondo screening.

DOI: 10.1103/PhysRevB.77.024409

PACS number(s): 75.30.Mb, 72.15.Qm, 75.30.-m

INTRODUCTION

The compound $\text{Yb}_{14}\text{MnSb}_{11}$ is a magnetically soft, low carrier concentration ferromagnet with a Curie temperature T_C of 53 ± 1 K. The compound was first synthesized by Chan *et al.*,¹ and the first single crystals were grown and characterized by Fisher *et al.*² X-ray absorption edge (XAS) and magnetic circular dichroism (XMCD) measurements³ found no evidence of magnetism associated with Yb, and concluded that Yb has a nonmagnetic Yb^{+2} configuration (filled $4f$ shell). This conclusion is supported by the observation of ferromagnetism at about 60 K in the isostructural compound $\text{Ca}_{14}\text{MnSb}_{11}$.¹ Low temperature magnetization measurements^{2,4} and XAS and XMCD data³ suggest a Mn^{+2} (d^5) configuration with the moment of one spin compensated by the antialigned spin of an Sb $5p$ hole. This configuration is consistent with the observed saturation magnetization at 2 K of $4\mu_B/\text{Mn}$.^{2,4} A d^5+h configuration is expected from electronic structure calculations on the related $\text{Ca}_{14}\text{MnBi}_{11}$ compounds⁵ and a d^5+h configuration is also found⁶ in the most heavily studied dilute magnetic semiconductor (DMS) GaAs:Mn. Good thermoelectric properties at elevated temperature have been reported recently for polycrystalline $\text{Yb}_{14}\text{MnSb}_{11}$ samples.⁷

Our original motivation for synthesizing large crystals of $\text{Yb}_{14}\text{MnSb}_{11}$ was to investigate the magnetism in a model DMS system. The ferromagnetic compound contains 3.8 at. % Mn with nearly one carrier per Mn. Each Mn is at a well-defined crystallographic site in the structure with a minimum Mn-Mn separation of 1 nm. Unlike many of the DMS alloys investigated in the literature, clustering of magnetic ions does not occur in this compound. On the basis of optical and thermodynamic measurements, Burch *et al.*⁸ were the first to suggest that the ferromagnetic ground state

of $\text{Yb}_{14}\text{MnSb}_{11}$ is unusual. They proposed that $\text{Yb}_{14}\text{MnSb}_{11}$ is a rare example of an underscreened Kondo lattice, with a Kondo temperature $T_K \approx 300$ K. As the material is cooled from high temperatures, part of the entropy associated with each Mn^{+2} $S=5/2$ spin is removed via ferromagnetic ordering and part is transferred via hybridization with the itinerant Sb $5p$ states near the Fermi energy, resulting in a renormalization of the density of states and an increase in the carrier effective mass. Optical measurements⁸ and heat capacity data down to 0.3 K (Ref. 4) give values for the electronic specific coefficient γ of about 160 mJ/mole K² and an effective mass $m^* \approx 20m_e$. Seebeck and resistivity measurements under pressure and chemical doping studies are also consistent with an underscreened Kondo lattice ground state.^{4,9} This unusual ground state depends on a delicate balance between carrier mediated magnetic order and a nonmagnetic Kondo ground state.¹⁰⁻¹³ Some unique aspects of the anomalous Hall data presented in this paper may be related to this delicate balance.

Our initial Hall experiments on $\text{Yb}_{14}\text{MnSb}_{11}$ were aimed only at estimating the carrier concentration, not a study of the anomalous Hall effect. In the course of the Hall measurements, however, it became clear that there were some distinct advantages of studying the anomalous Hall effect (AHE) in these types of low-carrier-concentration magnetically soft ferromagnetic materials known as Zintl compounds.^{14,15} The low carrier concentration ($\approx 10^{21}$ cm⁻³) and small magnetic anisotropy make it easier to measure and separate the normal and anomalous Hall contributions on thinned single crystals with different crystallographic orientations. A preliminary report of the AHE in three such ferromagnetic compounds [$\text{Yb}_{14}\text{MnSb}_{11}$ ($\mathbf{I} \parallel \mathbf{c}, \mathbf{H} \parallel \mathbf{a}$), $\text{Eu}_8\text{Ga}_{16}\text{Ge}_{30}$, and $\text{EuFe}_4\text{Sb}_{12}$] has been published.¹⁶

In the present paper, we focus on the orientation dependence of the AHE from single crystals of the tetrago-

nal compound $\text{Yb}_{14}\text{MnSb}_{11}$. Because the AHE data from $\text{Yb}_{14}\text{MnSb}_{11}$ in one geometry ($\mathbf{H}\parallel\mathbf{c}, \mathbf{I}\parallel\mathbf{a}$) is so unusual and unexpected, we also present AHE data from single crystals of two “normal” reference compounds $\text{EuFe}_4\text{Sb}_{12}$ ($T_C \approx 84$ K) and $\text{Yb}_{13.3}\text{La}_{0.7}\text{MnSb}_{11}$ ($T_C \approx 40$ K).

SYNTHESIS AND EXPERIMENTAL METHODS

Single crystals of $\text{Yb}_{14}\text{MnSb}_{11}$, $\text{Yb}_{13.3}\text{La}_{0.7}\text{MnSb}_{11}$, and $\text{EuFe}_4\text{Sb}_{12}$ are grown from molten metal fluxes.¹⁷ The 14-1-11 crystals are grown from a Sn flux using a method similar to that reported by Fisher *et al.*² with initial molar compositions for Yb:Mn:Sb:Sn of 14:5:11:90 and Yb:La:Mn:Sb:Sn of 12:2:5:11:90. If the Mn molar concentration is lowered to near 1, large crystals of another phase grew, namely, $\text{Yb}_{11}\text{Sb}_{10}$:Mn or $\text{Yb}_{11}\text{MnSb}_9$. Single crystals of the filled skutterudite $\text{EuFe}_4\text{Sb}_{12}$ are grown from an Sb flux with a starting composition of Eu:Fe:Sb of 1:4:20 as described previously.¹⁸ Energy dispersive x-ray analysis and x-ray structure refinements of the 14-1-11 crystals indicate that La only substituted for Yb, and that there was no evidence of antisite disorder; i.e., all of the Mn is confined to a unique crystallographic site and there is no mixing of Yb on Sb sites.⁴ Structure refinement of the $\text{EuFe}_4\text{Sb}_{12}$ crystals indicates fewer than 5% of vacancies on the Eu site, in agreement with previous data.¹⁸ The $\text{EuFe}_4\text{Sb}_{12}$ crystals grew as 3–5 mm size cubes, reflecting the underlying cubic crystal structure ($Im\bar{3}$, $a=0.917$ nm, 34 atoms per conventional unit cell). The 14-1-11 phase is tetragonal ($I41/acd$, $a=1.661$ nm, $c=2.195$ nm, 208 atoms per conventional unit cell), but the crystals have multiple faces and no simple growth habit (Fig. 1). The La doped 14-1-11 crystals have a similar growth habit and lattice parameters ($a=1.661$ nm and $c=2.199$ nm). Hall resistivity, electrical resistivity, and magnetoresistance measurements were made on thinned single crystal plates using the resistivity option, and horizontal rotator option for a physical property measurement system from Quantum Design. Six 0.025-mm-diameter Pt wire leads were attached to each crystal using H20E silver epoxy from EpoTek. The 14-1-11 crystals were lightly sanded before attaching the leads. The epoxy was cured at 373 K in a nitrogen atmosphere to avoid oxidation of the sample surface. Typical contact resistance was less than 5 Ω . For the Hall resistivity measurements, any voltages due to a misposition of the Hall leads were corrected by either reversing the direction of the magnetic field or by rotating the crystal by 180° in a fixed magnetic field. As in any Hall measurement, only voltages that are an odd function of the magnetic field were kept. Magnetization data were collected using a commercial superconducting quantum interference device magnetometer from Quantum Design.

RESULTS

Typical Hall resistivity data from single crystals of $\text{Yb}_{14}\text{MnSb}_{11}$ in two orientations are shown in Fig. 2. The data are from two different crystals that were oriented and polished into a thin plate. Three crystals in each orientation were examined to ensure that the results were due to the

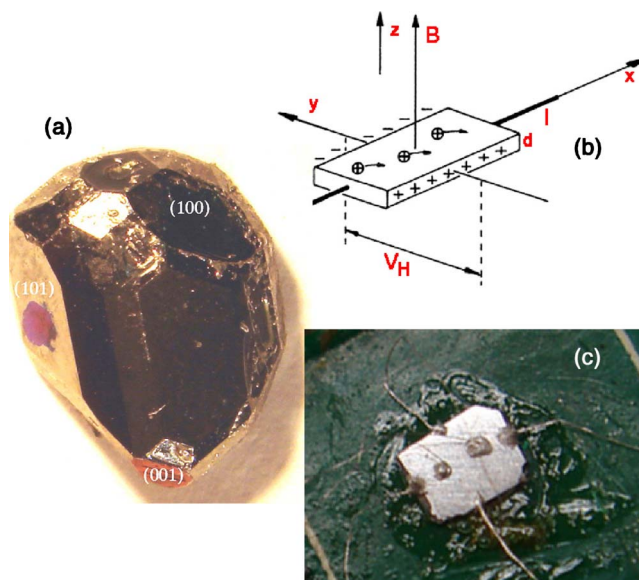


FIG. 1. (Color online) (a) Crystal of $\text{Yb}_{14}\text{MnSb}_{11}$ illustrating the unusual growth habit. Several of the facets are identified using x-ray diffraction. The as-grown crystal weighed 0.67 g. (b) A schematic of the geometry used for the Hall measurements. In the rotation experiments, the sample is tilted about the y axis. (c) Hall and resistivity leads attached to a crystal that is thinned and ground into a rectangular plate measuring about $3 \times 4 \times 0.7$ mm³ and weighing 80 mg.

orientation of the crystal and not to the slight variations in properties among crystals from different growth batches. For a magnetic material, the Hall resistivity is normally described by $\rho_{xy} = R_0 B + \rho'_{xy}$, where $R_0 B$ is the ordinary contribution and ρ'_{xy} describes the anomalous contribution to the AHE. The Hall coefficient R_0 is inversely proportional to the carrier concentration in simple doped semiconductors. In many materials ρ'_{xy} is proportional to the magnetization M and is often written as $\rho'_{xy} \approx R_s 4\pi M$.^{19–21} In general, however, ρ'_{xy} is a more complicated function of M that can in principle be determined from the electronic structure.^{22–29} In the limit of zero applied magnetic field, ρ'_{xy} can be parametrized^{30,16,21} by $\rho'_{xy} = [\sigma'_{xy} \rho^2 + a\rho] f[M(T)/M(0)]$, where ρ is the zero field resistivity $\rho_{xx}(H \approx 0)$, σ'_{xy} is the intrinsic anomalous Hall conductivity, a describes the extrinsic contribution from skew scattering, and f is a general function of the spontaneous magnetization $M(T)$. At low temperatures ($T \ll T_C$), the spontaneous magnetization saturates and $f[M(T)/M(0)] \approx 1$, while for $T > T_C$, $f[M(T)/M(0)] = 0$. To be consistent with the notation used in most theoretical calculations, we set $\sigma'_{xy} = \sigma_{xy} \approx \sigma_{xy}^0$, where σ_{xy}^0 is the anomalous Hall conductivity in the limit $T \ll T_C$. The limited theoretical calculations^{21,26} to date on a variety of different materials indicate σ_{xy} is at most a very weak function of temperature and hence we approximate it by its low temperature value σ_{xy}^0 . The skew scattering coefficient a is also assumed to be independent of temperature. With these approximations the anomalous Hall resistivity in the limit of zero applied magnetic field is described by

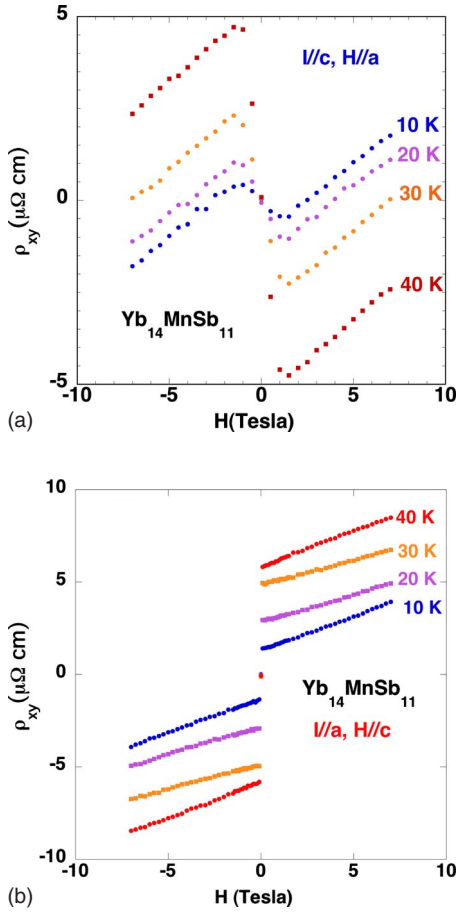


FIG. 2. (Color online) (a) Hall data from a $\text{Yb}_{14}\text{MnSb}_{11}$ crystal with $\mathbf{H}\parallel\mathbf{a}$ and $\mathbf{I}\parallel\mathbf{c}$. For clarity, only a portion of the Hall data is shown. For positive values of magnetic field ($H > 2$ T) the extrapolated intercepts at $H=0$ are negative. The extrapolated intercept at $H=0$ is defined as ρ'_{xy} , the anomalous Hall resistivity in the limit of zero applied magnetic field. These data are similar to those reported previously by us on another $\text{Yb}_{14}\text{MnSb}_{11}$ crystal with $\mathbf{I}\parallel\mathbf{c}$ and $\mathbf{H}\parallel(110)$ direction (see Fig. 8 of Ref. 16). (b) Hall data from a $\text{Yb}_{14}\text{MnSb}_{11}$ crystal with $\mathbf{H}\parallel\mathbf{c}$ and $\mathbf{I}\parallel\mathbf{a}$. For clarity, only a portion on the Hall data is shown. For positive values of magnetic field ($H > 2$ T), the extrapolated intercepts at $H=0$ are positive, opposite to that found in Fig. 2(a).

$$\rho'_{xy} = [\sigma_{xy}^0 \rho^2 + a^0 \rho][M(T)/M(0)], \quad (1)$$

where we have also assumed the simplest approximation for f , i.e., $f[M(T)/M(0)] = M(T)/M(0)$. The experimental value of ρ'_{xy} is determined by extrapolating the Hall resistivity data, such as shown in Fig. 2, from higher magnetic fields back to $H=0$. Since only small magnetic fields are required to align the magnetic domains, and since the normal portion of the Hall resistivity is rather large, this extrapolation is straightforward. However, we note that in some materials, such as MnSi, this procedure is complicated by a large magnetoresistance and a high carrier concentration.³¹ The magnetoresistance $\rho_{xx}(H, T)$ is shown in Fig. 3 for both orientations. Although at high fields and for temperatures near T_C , ρ_{xx} changes by as much as 25%, the estimated error in extrapo-

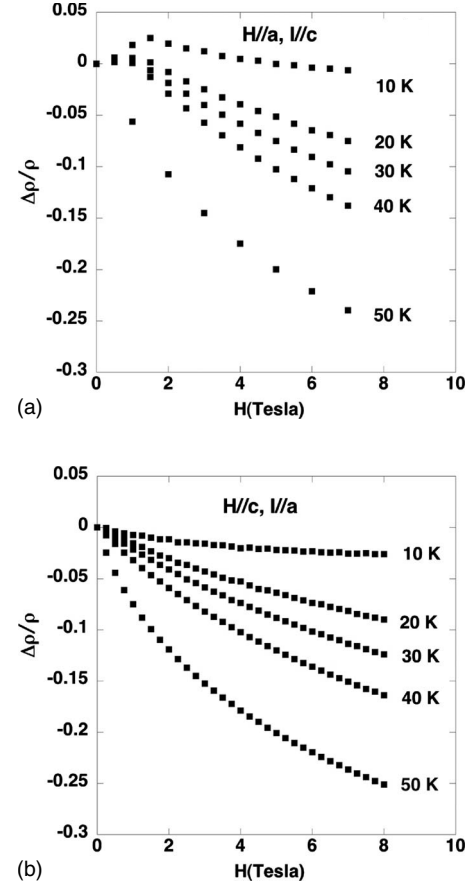


FIG. 3. (a) Magnetoresistance $[\rho_{xx}(H=0) - \rho_{xx}(H)] / \rho_{xx}(H=0)$ of $\text{Yb}_{14}\text{MnSb}_{11}$ crystals at the indicated temperatures for (a) $\mathbf{H}\parallel\mathbf{a}$ and $\mathbf{I}\parallel\mathbf{c}$ and (b) $\mathbf{H}\parallel\mathbf{c}$ and $\mathbf{I}\parallel\mathbf{a}$.

lating Hall resistivity data back to $H=0$ to obtain ρ'_{xy} is less than 2%. This is because most of the linear slope in the Hall resistivity [see Figs. 2(a) and 2(b)] is due to the normal Hall effect. The most obvious difference in the data shown in Figs. 2(a) and 2(b) is a change in the sign of ρ'_{xy} . In Fig. 2(a), ($\mathbf{H}\parallel\mathbf{a}, \mathbf{I}\parallel\mathbf{c}$) ρ'_{xy} is negative for all temperatures, while for ($\mathbf{H}\parallel\mathbf{c}, \mathbf{I}\parallel\mathbf{a}$) ρ'_{xy} is positive for all temperatures [Fig. 2(b)]. To our knowledge, this is the first example in which the sign of the AHE depends on the crystallographic orientation. The sign change persists in finite magnetic fields to temperatures well above T_C , as illustrated in Fig. 4. The carrier concentration for each crystal is estimated from Hall resistivity data at 5 K to be $1.6 \pm 0.1 \times 10^{21}$ holes/cm³, which corresponds to about one hole per Mn. These values are similar to those reported by us previously,¹⁶ and to the high temperature values reported by Brown *et al.*⁷ for a polycrystalline sample.

The anomalous Hall resistivity in the limit of zero applied magnetic field is analyzed using Eq. (1). The experimental quantities ρ'_{xy} , ρ , and $M(T)/M(0)$ were measured at each temperature $T < T_C$. The intrinsic Hall conductivity σ_{xy}^0 and the skew scattering coefficient a^0 are determined by fitting a line to plots of $[M(0)/M(T)] \rho'_{xy} / \rho$ versus ρ . The slope of the line yields σ_{xy}^0 and the intercept a^0 . Using the data shown in Fig. 2(a), along with the measured resistivity and spontaneous magnetization data (see Ref. 16 for more details), results

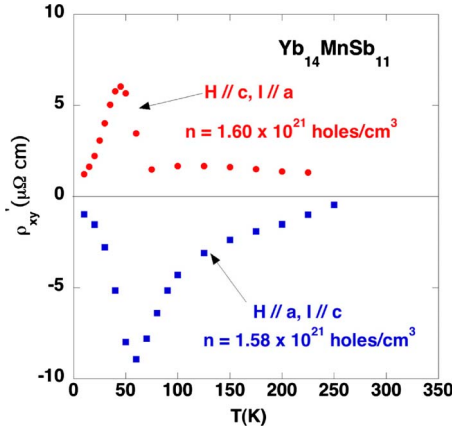


FIG. 4. (Color online) Anomalous Hall resistivity at 7 T vs temperature. The carrier concentration at 5 K was estimated for each crystal and assumed to be approximately constant at higher temperatures.

in values of $\sigma_{xy}^0 = -32 \pm 1 \Omega^{-1} \text{cm}^{-1}$ and $a^0 = -0.0037$ [Fig. 5(a)]. These values have the same sign and magnitude found before¹⁶ with $\mathbf{H} \parallel (110)$, $\mathbf{I} \parallel c$ ($\sigma_{xy}^0 = -33 \pm 1 \Omega^{-1} \text{cm}^{-1}$, $a^0 = -0.0049$, note that these are the correct values; there is an error in Ref. 16 where the incorrect geometrical factor was entered for ρ_{xx}). Analysis of the Hall data with $\mathbf{H} \parallel c$ and $\mathbf{I} \parallel a$, however, results in qualitatively different behaviors unlike any we have observed in our investigations of a variety of ferromagnets. Using the data, part of which is displayed in Fig. 2(b), and using as before Eq. (1) to analyze the data result in the analysis displayed in Fig. 5(b). This analysis of the AHE clearly fails for this crystal orientation. Similar behavior was found on two other $\text{Yb}_{14}\text{MnSb}_{11}$ crystals with the same Hall geometry. One or more of the assumptions used to parametrize ρ'_{xy} is clearly not valid for this orientation of the crystal.

To help understand the unusual behavior shown in Fig. 5(b), we examined the AHE from chemically doped crystals of $\text{Yb}_{14}\text{MnSb}_{11}$, namely, $\text{Yb}_{13.3}\text{La}_{0.7}\text{MnSb}_{11}$. The replacement of Yb^{+2} by La^{+3} ions tends to reduce the hole concentration, introduce some chemical disorder, and reduce the screening of the Mn^{+2} moments.⁴ These crystals are ferromagnetic with $T_C \approx 42 \pm 2$ K, depending on the exact growth conditions, have a lower carrier concentration, a higher saturation magnetization, and a much higher residual resistivity for $T \ll T_C$ (Fig. 6). Because of a smaller change in ρ below T_C (Fig. 6), the Hall resistivity does not vary much with temperature [Fig. 7(a)]. Analysis of these data [Fig. 7(b)] from the La doped crystals with $\mathbf{H} \parallel c$ and $\mathbf{I} \parallel a$, however, reveals a conventional dependence of the AHE on temperature and resistivity, in sharp contrast to the behavior exhibited by the undoped crystals [Fig. 5(b)]. Hall data from the La doped crystals with $\mathbf{H} \parallel a$ and $\mathbf{I} \parallel c$ (not shown) exhibit negative values of ρ'_{xy} indicating a change in sign of the AHE with crystal orientation for both the doped and undoped crystals.

Single crystals of the tetragonal ferromagnets $\text{Yb}_{14}\text{MnSb}_{11}$ and $\text{Yb}_{13.3}\text{La}_{0.7}\text{MnSb}_{11}$ both exhibit a change in sign of the anomalous Hall resistivity ρ'_{xy} , depending on the orientation of the crystal. With $\mathbf{H} \parallel c$ and $\mathbf{I} \parallel a$, ρ'_{xy} is positive,

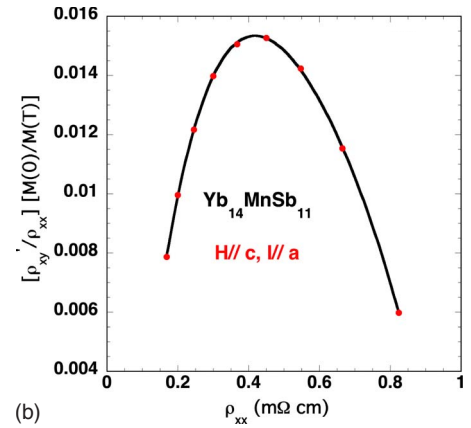
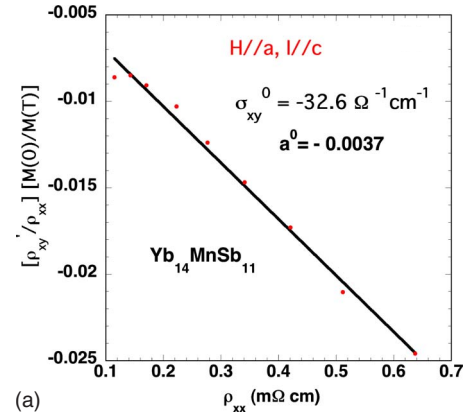


FIG. 5. (Color online) (a) Analysis of the intrinsic and extrinsic contributions to the AHE of an $\text{Yb}_{14}\text{MnSb}_{11}$ crystal with $\mathbf{H} \parallel a$ and $\mathbf{I} \parallel c$. The approximation of $\rho'_{xy} = (\sigma_{xy}^0 \rho^2 + a^0 \rho) [M(T)/M(0)]$ is used to analyze the data. (b) Attempted analysis of the intrinsic and extrinsic contributions to the AHE of an $\text{Yb}_{14}\text{MnSb}_{11}$ crystal with $\mathbf{H} \parallel c$ and $\mathbf{I} \parallel a$. The line through the data is a guide to the eye.

while when $\mathbf{H} \parallel a$ and $\mathbf{I} \parallel c$, ρ'_{xy} is negative. The temperature dependence of the anomalous Hall resistivity behaves normally except for the undoped crystal with $\mathbf{H} \parallel c$ and $\mathbf{I} \parallel a$ [see Fig. 5(b)]. To explore this unusual behavior, we examined the effects of tilting the sample with respect to the magnetic field on the measured Hall resistivity. Referring to Fig. 1(b), the sample was rotated around the y axis by an angle Θ . The Hall voltage is corrected for any offset of the Hall leads by reversing the applied magnetic field and only keeping voltages that are odd in the magnetic field. These crystals are soft ferromagnets which means that for fields larger than about 2 T, the applied magnetic field \mathbf{H} and the magnetization \mathbf{M} of the sample point in the same direction. This is illustrated in Fig. 8 where the magnetization of one of the undoped $\text{Yb}_{14}\text{MnSb}_{11}$ crystals is shown as a function of the angle between the easy c axis and the applied magnetic field. Similar magnetization results are found for the La doped crystals. As the crystal is rotated around the y axis by an angle Θ , the component of \mathbf{H} perpendicular to the current \mathbf{I} is $\mathbf{H} \cos \Theta$, and if $\mathbf{H} > 2$ T, the component of \mathbf{M} perpendicular to \mathbf{I} is $\mathbf{M} \cos \Theta$.

Typical Hall resistivity data below T_C for a $\text{Yb}_{14}\text{MnSb}_{11}$ crystal that is rotated with respect to the applied magnetic

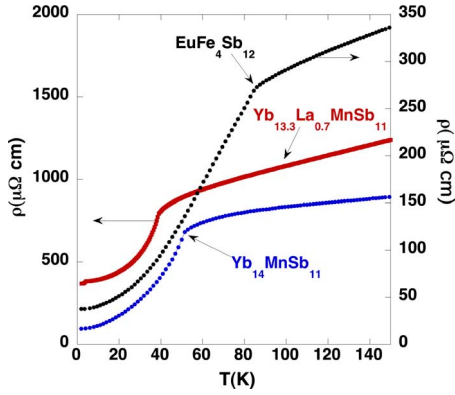
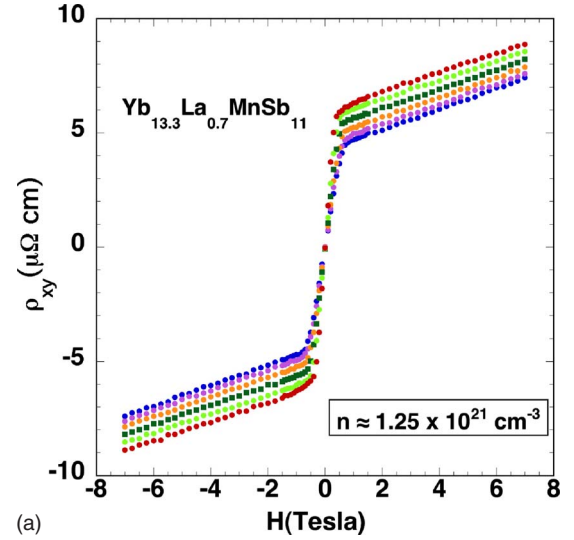


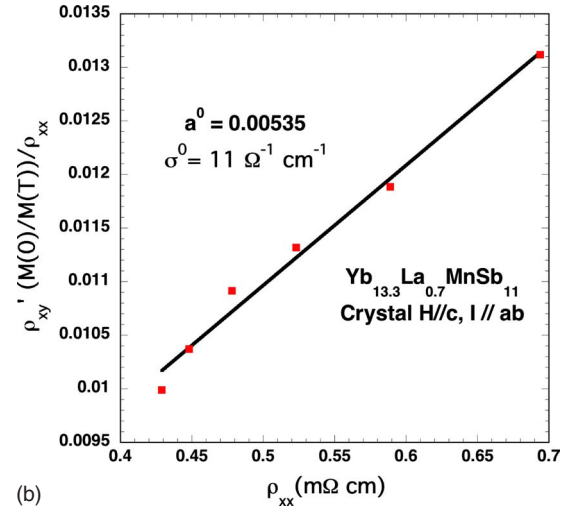
FIG. 6. (Color online) Resistivity versus temperature for three ferromagnets. The left resistivity scale is for the La doped and undoped 14-1-11 crystals. Note the relatively small decrease in the resistivity of the La doped crystal below $T_C \approx 40$ K. The resistivity data for each crystal are recorded during the Hall measurements using two additional leads near the center of the rectangular plate [see Fig. 1(c)]. Although this is not the best geometry for determining the absolute values of the resistivity, this method eliminates variations in resistivity among different crystals. The absolute values of the resistivity are only accurate to within about 20%, mainly due to the uncertainty in the geometry of the leads. The resistivity data in the figure are associated with the Hall data displayed in Figs. 5(a), 7, and 12.

field is shown in Fig. 9(a). With 0° rotation $\mathbf{H} \parallel \mathbf{c}$ and $\mathbf{I} \parallel \mathbf{a}$. As the sample is rotated about the y axis by Θ , the slope of the Hall resistivity data in finite magnetic fields decreases approximately as $\cos \Theta$ [see Fig. 9(b)]. This is expected since the slope is primarily due to the normal Hall effect and the Lorentz force depends on the component of \mathbf{B} perpendicular to \mathbf{I} , i.e., $\mathbf{B} \cos \Theta \approx \mathbf{H} \cos \Theta$ (for the 14-1-11 crystals, $4\pi\mathbf{M}_{\text{sat}}$ is only 600 G). The value of the anomalous Hall resistivity ρ'_{xy} , however, does not depend on the angle of rotation for rotation angles up to at least 80° . This result is so unexpected, that we repeated the measurements on two other $\text{Yb}_{14}\text{MnSb}_{11}$ crystals with the same orientation ($\mathbf{H} \parallel \mathbf{c}$ and $\mathbf{I} \parallel \mathbf{a}$) and for various temperatures well below T_C . The conclusion is the same; in this orientation, ρ'_{xy} does not depend on the angle of rotation. Since \mathbf{M} essentially follows the direction of the applied field (see Fig. 8), this means that within our experimental resolution, ρ'_{xy} does not depend on the direction of \mathbf{M} . To illustrate how unusual and unexpected this result is, we present several examples of “normal” behavior.

The same rotation experiments were performed on a pure undoped $\text{Yb}_{14}\text{MnSb}_{11}$ crystal but with $\mathbf{H} \parallel \mathbf{a}$ and $\mathbf{I} \parallel \mathbf{c}$ [crystal used for Figs. 2(a) and 5(a)], a La doped crystal with $\mathbf{H} \parallel \mathbf{c}$ and $\mathbf{I} \parallel \mathbf{a}$ (crystal used for Fig. 7), and an $\text{EuFe}_4\text{Sb}_{12}$ crystal (resistivity data shown in Fig. 6). Some results from these experiments are displayed in Figs. 10–12. For all three crystals, ρ'_{xy} decreases approximately as $\cos(\Theta)$ when the applied magnetic field and magnetization are rotated by an angle Θ with respect to the direction of the current through the crystal.



(a)



(b)

FIG. 7. (Color online) (a) Hall resistivity vs field with $\mathbf{H} \parallel \mathbf{c}$ and $\mathbf{I} \parallel \mathbf{a}$ for a La doped crystal for temperatures between 35 and 10 K. (b) Analysis of the intrinsic and extrinsic contributions to the AHE using Eq. (1) to analyze these data.

DISCUSSION

The anomalous Hall resistivity of ferromagnets ρ'_{xy} is usually described as originating from two sources: an extrinsic contribution due to skew scattering^{32,33} that is proportional to ρ and an intrinsic contribution^{19,22} proportional to ρ^2 . A contribution to ρ'_{xy} proportional to ρ^2 is intrinsic in the sense that the more fundamental Hall conductivity, $\sigma_{xy} \approx \rho_{xy}/\rho^2$ (just from inverting the resistivity tensor), becomes independent of scattering. The seminal work of Karplus and Luttinger²² showed that the intrinsic contribution originated from the spin-orbit coupling of Bloch bands, which in principle could be determined from careful calculations of the electronic structure. Berry³⁴ showed that this type of intrinsic contribution is a very general consequence of the application of quantum mechanics to condensed matter systems that do not have either time reversal invariance (a ferromagnet, for example) or inversion symmetry (many crystal structures lack

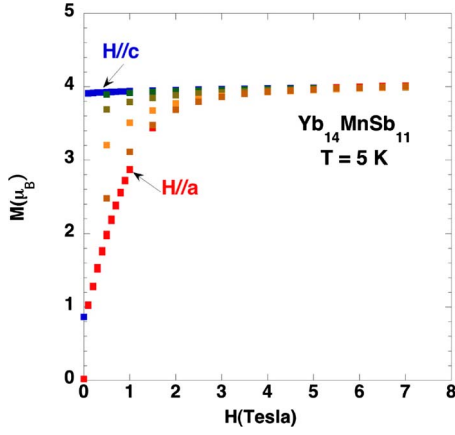


FIG. 8. (Color online) Magnetization versus applied magnetic field. Data are shown with $\mathbf{H}\parallel c$, and with the sample rotated toward the a axis by 20° , 40° , 60° , 80° , and 90° ($\mathbf{H}\parallel a$). For fields larger than about 2 T, the sample magnetization \mathbf{M} is aligned along the direction of the applied magnetic field \mathbf{H} .

inversion symmetry). The insight provided by Berry on the consequence of Berry phase effects on Bloch electrons in condensed matter systems has stimulated several groups to calculate the intrinsic anomalous Hall conductivity both at $T=0$ and as a function of temperature. Calculations of the intrinsic Hall conductivity from simple ferromagnets,²⁶ such as Fe, have shown that the sign and the magnitude of σ_{xy} are dominated by “hot spots” in the electronic structure and that there is no simple relationship between σ_{xy} and the sign of the normal Hall coefficient. It is then perhaps not too surprising that for a complex tetragonal ferromagnet such as $\text{Yb}_{14}\text{MnSb}_{11}$ with 208 atoms in the conventional unit cell that the sign of σ_{xy} is different depending on whether the current is along c or a . We note, however, that to our knowledge, this is the first compound where the sign of σ_{xy} depends on the orientation of the crystal. Although detailed calculations of the intrinsic Hall conductivity are probably not feasible at the present time for $\text{Yb}_{14}\text{MnSb}_{11}$, the approximate magnitude³⁵ of σ_{xy} should be given by $|\sigma_{xy}| \approx 0.1e^2k_F/h \approx 100 \Omega^{-1} \text{cm}^{-1}$, as compared with the measured value of $|\sigma_{xy}| = 33 \Omega^{-1} \text{cm}^{-1}$ [see Fig. 5(a)]. The data in Fig. 5(b) are more difficult to understand. While a sign change with crystal direction can be rationalized within the Berry scenario of the AHE, the completely different functional dependence of ρ'_{xy} on ρ and M when $\mathbf{I}\parallel a$ and $\mathbf{H}\parallel c$ is puzzling since the resistivity is not very anisotropic (i.e., $\rho_c/\rho_a \approx 1.4$), the magnetic susceptibility well above T_C is isotropic, and the ferromagnetism is fairly soft. In this same geometry ($\mathbf{I}\parallel a$), if the direction of the \mathbf{M} is rotated by an angle Θ such that the component of \mathbf{M} perpendicular to \mathbf{I} is $\mathbf{M} \cos(\Theta)$, ρ'_{xy} remains unchanged (see Fig. 9). This means that in this geometry ρ'_{xy} does not depend on the direction of \mathbf{M} . There may be other ferromagnetic compounds where this is true, but the tilting experiments are not normally done in most Hall studies, and we are not aware of other examples. The expected behavior for ρ'_{xy} is recovered, however, if a small amount of the nonmagnetic Yb^{+2} is replaced by nonmagnetic La^{+3} (i.e., $\text{Yb}_{13.3}\text{La}_{0.7}\text{MnSb}_{11}$). A small amount of

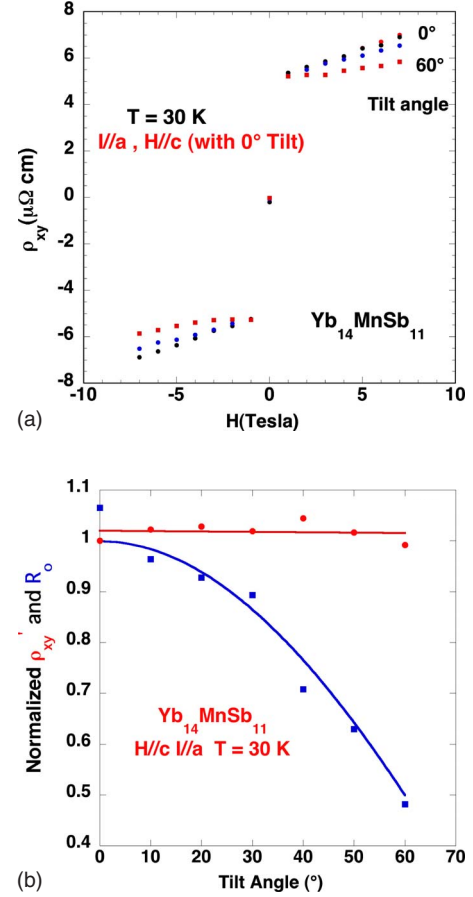


FIG. 9. (Color online) (a) Hall resistivity data at 30 K from a $\text{Yb}_{14}\text{MnSb}_{11}$ for various rotation angles about the y axis [see Fig. 1(b)]. The crystal is prepared with $\mathbf{I}\parallel a$ and $\mathbf{H}\parallel c$ for 0 tilt angle. Note that ρ'_{xy} is essentially independent of tilt angle. (b) Analysis of Hall resistivity data, a portion of which is displayed in Fig. 8(a). The slope of the Hall resistivity data for $H > 0.5$ T is defined as R_0 . The variation R_0 with tilt angle is fit to $R_N \cos \Theta$. Squares are R_0/R_N and blue line is $\cos \Theta$. The normalized anomalous Hall resistivity is defined as $\rho'_{xy}(\Theta)/\rho'_{xy}(0)$. The red line is a least squares fit to the AHE data.

chemical alloying is apparently enough to destroy the unique features of the ground state observed in the undoped $\text{Yb}_{14}\text{MnSb}_{11}$ compound. As discussed in the Introduction, there is strong evidence that $\text{Yb}_{14}\text{MnSb}_{11}$ is a rare example of an underscreened Kondo lattice with a Kondo temperature $T_K \approx 300$ K.^{4,8} This unusual ground state depends on a delicate balance between carrier mediated magnetic order and Kondo screening. It seems likely that some of the unique aspects of the anomalous Hall data presented in Figs. 5(b) and 9 are related to the interplay between Kondo physics and Berry phase effects. Since the data shown in Figs. 5(b) and 9 indicate a different dependence of ρ'_{xy} on ρ and M , the data in Fig. 5(b) are replotted in Fig. 13(a) and fit to a polynomial of the form $\rho'_{xy} = a + b\rho + c\rho^2$. A good fit to the data is obtained with $a = -4.33 \mu\Omega \text{cm}$, $b = 0.0389$, and $c = -37.5 \Omega^{-1} \text{cm}^{-1}$. The coefficient of the ρ^2 term is quite close to the value obtained for σ_{xy} from the “normal” crystal orientation [Fig. 5(a)]. This suggests that when $\mathbf{I}\parallel a$ and $\mathbf{H}\parallel c$ there is an ad-

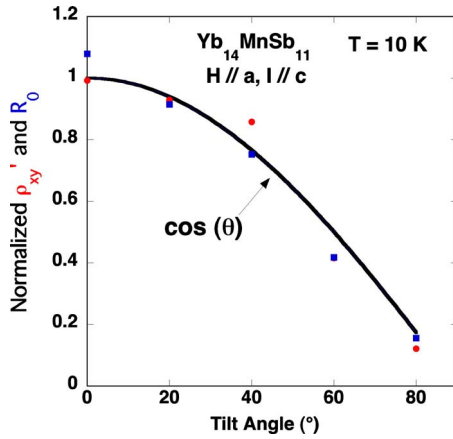


FIG. 10. (Color online) Effect of the rotation of a $\text{Yb}_{14}\text{MnSb}_{11}$ crystal ($\mathbf{I}\parallel\mathbf{c}$, and $\mathbf{H}\parallel\mathbf{a}$ for 0 tilt) about the y axis on the normal and anomalous contributions to the Hall resistivity. Both contributions approximately decrease as $\cos(\theta)$.

ditional large and positive contribution to ρ'_{xy} that is not present when $\mathbf{I}\parallel\mathbf{c}$ and $\mathbf{H}\parallel\mathbf{a}$. The additional contribution is linear in ρ with an offset of $-4.33 \mu\Omega \text{ cm}$, as shown in Fig. 13(b). If a residual resistivity ρ_0 of $110 \mu\Omega \text{ cm}$ is subtracted from the resistivity, the additional contribution is linear in $(\rho - \rho_0)$. In heavy fermion or Kondo-lattice compounds,^{36,37} both theory and experiment show a large contribution to the Hall resistivity that is proportional to $(\rho - \rho_0)$ times the magnetic susceptibility χ for temperatures well below T_K ($T_K \approx 300 \text{ K}$ for $\text{Yb}_{14}\text{MnSb}_{11}$).^{4,8} For a Kondo lattice system well below T_K , the susceptibility is essentially independent of temperature, which would make the portion of the Hall resistivity due to the Kondo effect proportional to $(\rho - \rho_0)$. In normal Kondo-lattice compounds (such as UPt_3),³⁶ of course ρ_{xy} and ρ'_{xy} are zero in the limit $H=0$, but for $\text{Yb}_{14}\text{MnSb}_{11}$, which is also ferromagnetic, the internal magnetic field that

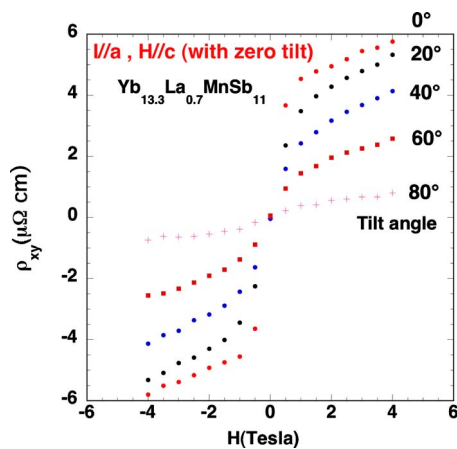


FIG. 11. (Color online) Hall resistivity data from a La doped $\text{Yb}_{14}\text{MnSb}_{11}$ crystal at 5 K with $\mathbf{I}\parallel\mathbf{a}$ and $\mathbf{H}\parallel\mathbf{c}$ for zero tilt angle. Note that both the intercept and the slope of the data for $H > 2 \text{ T}$ decrease as the sample are rotated about the y axis [see Fig. 1(b)] in contrast to the response of the pure $\text{Yb}_{14}\text{MnSb}_{11}$ crystal with the same orientation [see Fig. 8(a)].

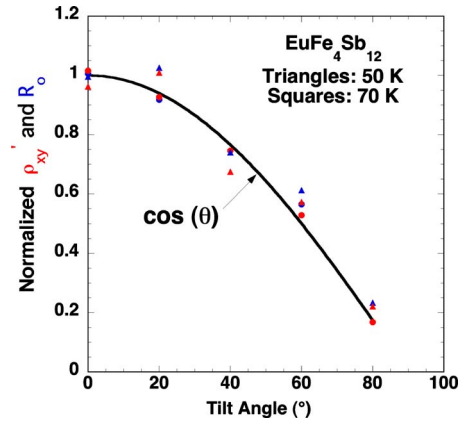


FIG. 12. (Color online) Effect of the rotation of a cubic $\text{EuFe}_4\text{Sb}_{12}$ crystal [$\mathbf{I}\parallel(100)$ and $\mathbf{H}\parallel(001)$ for 0 tilt] about the (010) axis on the normal and anomalous contributions to the Hall resistivity. Both contributions approximately decrease as $\cos(\theta)$. Hall resistivity data from two temperatures are shown.

develops below $T_C \approx 53 \text{ K}$ may result in an observable Kondo-like contribution to ρ'_{xy} that is linear in $(\rho - \rho_0)$. This is a plausible explanation for the large additional contribution linear in $(\rho - \rho_0)$ that is observed in Fig. 13.

We have considered a variety of different explanations for the unusual behavior of the Hall data from $\text{Yb}_{14}\text{MnSb}_{11}$ when $\mathbf{H}\parallel\mathbf{c}$ and $\mathbf{I}\parallel\mathbf{a}$. Preliminary neutron scattering data³⁸ from $\text{Yb}_{14}\text{MnSb}_{11}$ indicate a smooth, almost textbook increase of the magnetization order parameter as the temperature is lowered below T_C . There is no indication of a thermally induced spin reorientation and in zero applied field all of the Mn spins point along the \mathbf{c} axis. This same behavior is observed in magnetization measurements (see Fig. 3 of Ref. 16) as long as the applied field is large enough to produce a single magnetic domain sample. The field required to produce a monodomain sample is about 0.01 T when $\mathbf{H}\parallel\mathbf{c}$ (see Fig. 1 of Ref. 16) or 2 T when $\mathbf{H}\parallel\mathbf{a}$ (see Fig. 8). No magnetic hysteresis is observed between zero-field-cooled and field-cooled magnetization data for $H > 0.05 \text{ T}$. Therefore, for $\text{Yb}_{14}\text{MnSb}_{11}$, there is no experimental evidence of another Berry phase contribution to the AHE such as the spin chirality mechanism proposed for several pyrochlores,²⁸ or the Berry phase mechanism proposed for the manganites.³⁹ It is possible that the orientation dependence of the AHE in $\text{Yb}_{14}\text{MnSb}_{11}$ is due to a very unusual Fermi surface below T_C , but this speculation will have to await further theoretical insight. The simplest explanation that explains most of the $\text{Yb}_{14}\text{MnSb}_{11}$ data is a normal Berry phase contribution to the AHE, which is approximately the same in both orientations ($\sigma_{xy}^0 \approx -30 \Omega^{-1} \text{ cm}^{-1}$), and a skew scattering contribution that is highly anisotropic. The unusually large contribution to the AHE when $\mathbf{I}\parallel\mathbf{a}_0$ and $\mathbf{H}\parallel\mathbf{c}$ suggests that resonant Kondo skew scattering is important in this orientation. Exactly how this occurs in a ferromagnetic material is not known. Strong anisotropic skew scattering, however, is consistent with the theoretical calculations of Sanchez-Portal *et al.*⁵ who find highly directional magnetic coupling between Mn ions in a related ferromagnetic compound $\text{Ca}_{14}\text{MnSb}_{11}$. In “normal”

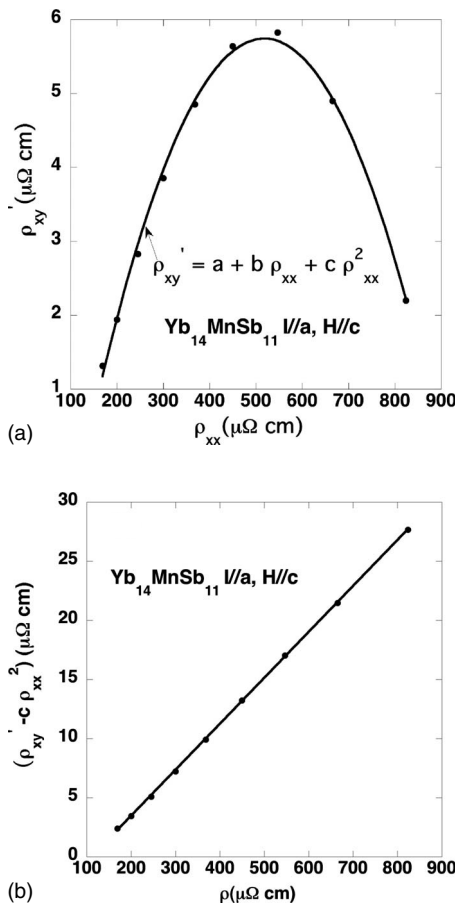


FIG. 13. (a) AHE effect data shown in Fig. 5(b) replotted as ρ'_{xy} vs ρ_{xx} . A simple polynomial in ρ_{xx} accurately describes the data with coefficients $a = -4.334 \mu\Omega \text{ cm}$, $b = 0.0389$, and $c = -37.5 \Omega^{-1} \text{ cm}^{-1}$. Note that the coefficient of ρ_{xx}^2 is surprisingly close to the value of $-32.6 \Omega^{-1} \text{ cm}^{-1}$ obtained from the $\text{Yb}_{14}\text{MnSb}_{11}$ crystal in Fig. 5(a). (b) Data in Fig. 13(a) with $-37.5\rho_{xx}^2$ subtracted from measured ρ'_{xy} values versus ρ_{xx} . The linear term approaches zero for $\rho_{xx} \approx 110 \mu\Omega \text{ cm}$, close to the residual resistivity value for this crystal. The large positive contribution to ρ'_{xy} proportional to $(\rho_{xx} - \rho_0)$ may be due to enhanced skew scattering associated with the Kondo effect.

Kondo lattice compounds, the skew scattering contribution is proportional to the susceptibility (rather than the magnetization), and it may be that the effective internal magnetic field present in the ferromagnetic state only has to be larger than a critical value for Kondo skew scattering to be effective. This might provide a qualitative explanation of the results from the tilting experiments shown in Fig. 9. Clearly, however, further theoretical insight is needed before one can claim that the Hall data from $\text{Yb}_{14}\text{MnSb}_{11}$ is understood.

CONCLUSIONS

The tetragonal compound $\text{Yb}_{14}\text{MnSb}_{11}$ is a rare example of an underscreened Kondo ferromagnet^{4,8,9} with $T_K \approx 300 \text{ K}$ and $T_C \approx 53 \text{ K}$. Each Mn^{2+} is at a well defined crystallographic site with a d^5 +hole electronic configuration⁵ similar to that found in $\text{GaAs}:\text{Mn}$.⁶ For $T < T_C$, the anomalous Hall resistivity ρ'_{xy} in the limit of zero applied magnetic field is negative when $\mathbf{H} \parallel \mathbf{a}$ and $\mathbf{I} \parallel \mathbf{c}$, and positive when $\mathbf{H} \parallel \mathbf{c}$ and $\mathbf{I} \parallel \mathbf{a}$. In both orientations, analysis of ρ'_{xy} yields an intrinsic Hall conductivity of $\sigma_{xy}^0 \approx -35 \Omega^{-1} \text{ cm}^{-1}$ but the skew scattering contributions differ by an order of magnitude: $a^0 = -0.0037$ when $\mathbf{H} \parallel \mathbf{a}$ and $\mathbf{I} \parallel \mathbf{c}$ and $a^0 = 0.0389$ when $\mathbf{H} \parallel \mathbf{c}$ and $\mathbf{I} \parallel \mathbf{a}$. The gigantic skew scattering observed with $\mathbf{H} \parallel \mathbf{c}$ is possibly due to resonant Kondo scattering, although why it is so large only in one orientation is not completely understood. When skew scattering dominates ($\mathbf{I} \parallel \mathbf{a}$), rotation of \mathbf{M} from $\mathbf{M} \parallel \mathbf{c}$ to $\mathbf{M} \approx \parallel \mathbf{I} \parallel \mathbf{a}$ does not change ρ'_{xy} implying that ρ'_{xy} does not depend on the direction of \mathbf{M} .

ACKNOWLEDGMENTS

It is a pleasure to acknowledge stimulating and illuminating discussions with Allan MacDonald, Qian Niu, Peter Khalifah, and Steve Nagler. Research sponsored by the Division of Materials Sciences and Engineering, Office of Basic Energy Sciences, U.S. Department of Energy under Contract No. DE-AC05-00OR22725 with Oak Ridge National Laboratory, managed and operated by UT-Battelle, LLC.

- ¹J. Y. Chan, M. M. Olmstead, S. M. Kauzlarich, and D. J. Webb, *Chem. Mater.* **10**, 3583 (1998).
- ²I. R. Fisher, T. A. Wiener, S. L. Budko, P. C. Canfield, J. Y. Chan, and S. M. Kauzlarich, *Phys. Rev. B* **59**, 13829 (1999).
- ³A. P. Holm, S. M. Kauzlarich, S. A. Morton, G. D. Waddill, W. E. Pickett, and J. G. Tobin, *J. Am. Chem. Soc.* **124**, 9894 (2002).
- ⁴B. C. Sales, P. Khalifah, T. P. Enck, E. J. Nagler, R. E. Sykora, R. Jin, and D. Mandrus, *Phys. Rev. B* **72**, 205207 (2005).
- ⁵D. Sanchez-Portal, R. M. Martin, S. M. Kauzlarich, and W. E. Pickett, *Phys. Rev. B* **65**, 144414 (2002).
- ⁶T. C. Schulthess, W. M. Temmerman, Z. Szotek, W. H. Butler, and G. M. Stocks, *Nat. Mater.* **4**, 838 (2005).
- ⁷S. R. Brown, S. M. Kauzlarich, F. Gascoin, and G. J. Snyder,

Chem. Mater. **18**, 1873 (2006).

- ⁸K. S. Burch, A. Schafgans, N. P. Butch, T. A. Sayles, M. B. Maple, B. C. Sales, D. Mandrus, and D. N. Basov, *Phys. Rev. Lett.* **95**, 046401 (2005).
- ⁹A. Akrap, N. Barisic, L. Forro, D. Mandrus, and B. C. Sales, *Phys. Rev. B* **76**, 085203 (2007).
- ¹⁰P. Fazekas, *Lecture Notes on Electron Correlation and Magnetism* (World Scientific, Singapore, 1999), p. 643.
- ¹¹S. Doniach, *Physica B & C* **91**, 231 (1977).
- ¹²A. L. Cornelius, A. K. Gangopadhyay, J. S. Schilling, and W. Assmus, *Phys. Rev. B* **55**, 14109 (1997).
- ¹³S. K. Malik and D. T. Adroja, *Phys. Rev. B* **43**, 6295 (1991).
- ¹⁴J. D. Corbett, *Chem. Rev. (Washington, D.C.)* **85**, 383 (1985).

- ¹⁵B. C. Sales, in *Handbook Phys. and Chem. Rare Earths: Filled Skutterudites*, edited by K. A. Gschneidner (Elsevier, New York, 2003), Vol. 33, Chap. 211, p. 1.
- ¹⁶B. C. Sales, R. Jin, D. Mandrus, and P. Khalifah, *Phys. Rev. B* **73**, 224435 (2006).
- ¹⁷M. G. Kanatzidis, R. Pottgen, and W. Jeitschko, *Angew. Chem., Int. Ed.* **44**, 6996 (2005).
- ¹⁸E. D. Bauer, A. Slebarski, N. A. Frederick, W. M. Yuhasz, M. B. Maple, D. Cao, F. Bridges, G. Geister, and P. Rogl, *J. Phys.: Condens. Matter* **16**, 5095 (2004).
- ¹⁹L. Berger and G. Bergmann, in *The Hall Effect and Its Applications*, edited by C. L. Chen and C. R. Westgate (Plenum, New York, 1980), Chap. 2, p. 55.
- ²⁰E. H. Hall, *Philos. Mag.* **12**, 157 (1881).
- ²¹C. G. Zeng, Y. G. Yao, Q. Niu, and H. H. Weitering, *Phys. Rev. Lett.* **96**, 037204 (2006).
- ²²R. Karplus and J. M. Luttinger, *Phys. Rev.* **95**, 1154 (1954).
- ²³Z. Fang, N. Nagaosa, K. S. Takahashi, A. Asamitsu, R. Mathieu, T. Ogasawara, H. Yamada, M. Kawasaki, Y. Tokura, and K. Terakura, *Science* **302**, 92 (2003).
- ²⁴R. Mathieu, A. Asamitsu, H. Yamada, K. S. Takahashi, M. Kawasaki, Z. Fang, N. Nagaosa, and Y. Tokura, *Phys. Rev. Lett.* **93**, 016602 (2004).
- ²⁵M. Onoda and N. Nagaosa, *J. Phys. Soc. Jpn.* **71**, 19 (2002).
- ²⁶Y. Yao, L. Kleinman, A. H. MacDonald, J. Sinova, T. Jungwirth, D. S. Wang, E. Wang, and Q. Niu, *Phys. Rev. Lett.* **92**, 037204 (2004).
- ²⁷I. V. Solovyev, *Phys. Rev. B* **67**, 174406 (2003).
- ²⁸Y. Taguchi, Y. Oohara, H. Yoshizawa, N. Nagaosa, and Y. Tokura, *Science* **291**, 2573 (2001).
- ²⁹T. Jungwirth, Q. Niu, and A. H. MacDonald, *Phys. Rev. Lett.* **88**, 207208 (2002).
- ³⁰J. Kotzler and W. Gil, *Phys. Rev. B* **72**, 060412(R) (2005).
- ³¹M. Lee, Y. Onose, Y. Tokura, and N. P. Ong, *Phys. Rev. B* **75**, 172403 (2007).
- ³²J. Smit, *Physica (Amsterdam)* **21**, 877 (1955).
- ³³J. Smit, *Physica (Amsterdam)* **24**, 39 (1958).
- ³⁴M. V. Berry, *Proc. R. Soc. London, Ser. A* **392**, 45 (1984).
- ³⁵A. H. MacDonald (private communication).
- ³⁶A. Fert and P. M. Levy, *Phys. Rev. B* **36**, 1907 (1987).
- ³⁷P. Coleman, P. W. Anderson, and T. V. Ramakrishnan, *Phys. Rev. Lett.* **55**, 414 (1985).
- ³⁸S. E. Nagler (private communication).
- ³⁹J. Ye, Y. B. Kim, A. J. Millis, B. I. Shraiman, P. Majumdar, and Z. Tesanovic, *Phys. Rev. Lett.* **83**, 3737 (1999).